Bioactive Materials 43 (2025) 330–339

Contents lists available at ScienceDirect

Bioactive Materials

journal homepage: www.keaipublishing.com/en/journals/bioactive-materials

Dexamethasone loaded DNA scavenger nanogel for systemic lupus erythematosus treatment

Haofang Zhu [a,b], Danqing Huang [b], Min Nie [b], Yuanjin Zhao [b,c,*], Lingyun Sun [a,b,**]

[a] Department of Rheumatology and Immunology, The First Affiliated Hospital of Anhui Medical University, Hefei, 230022, China
[b] Department of Rheumatology and Immunology, Institute of Translational Medicine, The Affiliated Drum Tower Hospital of Nanjing University Medical School, Nanjing, 210008, China
[c] State Key Laboratory of Bioelectronics, School of Biological Science and Medical Engineering, Southeast University, Nanjing, 210096, China

ARTICLE INFO

Keywords:
Peptide dendrimer
Nanogel
Targeting
Cell-free DNA
Lupus nephritis

ABSTRACT

Lupus nephritis (LN) poses a severe risk for individuals with systemic lupus erythematosus (SLE), prompting extensive research into targeted delivery systems capable of modulating immune responses and clearing cell-free DNA (cfDNA). Here, we propose a novel renal homing nanogel that acts as a cfDNA scavenger and a dexamethasone (DXM) delivery carrier for LN treatment. Based on the generation 3 polylysine dendrimers, the created cationic nanogels (G3DSP) exhibit minimal toxicity and outstanding DXM loading efficiency. Our studies confirm that these nanogels can competitively bind with anionic cfDNA *in vitro*, leading to the suppression of toll-like receptor 9 (TLR9) activation. When administered systemically to MRL/lpr mice, the nanogels preferentially localize to and are retained in the inflamed kidneys, releasing their payload in response to reactive oxygen species (ROS), therefore effectively ameliorating SLE symptoms. Consequently, G3DSP nanogels emerge as a promising effective combined therapy for LN, minimizing cfDNA accumulation in vital organs and delivering immunomodulatory benefits through DXM.

1. Introduction

Lupus nephritis (LN), a prevalent and potentially fatal complication of systemic lupus erythematosus (SLE) [1,2], involves complex immunological mechanisms, prominently featuring the production of anti-dsDNA antibodies and cell-free DNA (cfDNA) [3,4]. This cfDNA can aberrantly trigger endosomal toll-like receptors (TLRs), catalyzing a cascade of signaling events that lead to the unregulated production of proinflammatory autoantibodies [5–7]. Dexamethasone (DXM), a corticosteroid, is a cornerstone in LN management [8–10]. Through intravenous administration, DXM can demonstrate broad suppressive effects on the immune response and achieve disease remission [11–13]. However, due to systematic toxicity caused by the off-target effects, long-term employment of DXM is limited [14–17]. Furthermore, it is important to note that DXM alone is unable to eliminate the pathogenic cfDNA that disrupts innate immune tolerance during the progression of LN. Therefore, there is an urgent need for innovative approaches that can augment the therapeutic efficacy of DXM, minimize its adverse effects, and effectively clear cfDNA to halt the progression of LN.

Here, we proposed a novel inflamed kidney-targeting nanogel as DXM carrier and cfDNA scavenger to treat LN. In organisms, cell fragments and metabolic wastes can be cleared by organelles through ionic interactions [18–21]. For example, the cfDNA is a class of nucleic acid debris with negative charges, which can be recognized and absorbed by various organelles and bio-actives with positive charges [22–25]. Bases on this phenomenon, cfDNA-binding polymers have been extensively explored to dampen inappropriate TLR activation and combat inflammatory disorders [26–29]. As a natural biological polymer with positive charges, cationic peptide dendrimers have attracted increasing interest for their unique multivalency, function amplification capability, drug-loading property, intrinsic biocompatibility, and superior biodegradability [30–34]. They can transmigrate through various biological barriers and be easily ingested by cellular lysosomes, making them promising candidates for nanomedicine [35–39]. Additionally, nanogels

Peer review under responsibility of KeAi Communications Co., Ltd.
* Corresponding author. Department of Rheumatology and Immunology, Institute of Translational Medicine, The Affiliated Drum Tower Hospital of Nanjing University Medical School, Nanjing, 210008, China.
** Corresponding author. Department of Rheumatology and Immunology, The First Affiliated Hospital of Anhui Medical University, Hefei, 230022, China.
E-mail addresses: yjzhao@seu.edu.cn (Y. Zhao), lingyunsun@nju.edu.cn (L. Sun).

https://doi.org/10.1016/j.bioactmat.2024.08.030
Received 11 June 2024; Received in revised form 9 August 2024; Accepted 27 August 2024
Available online 28 September 2024

are a type of hydrogel that has been widely utilized as drug carriers in various biomedical applications [40–44]. Thus, it is conceivable that the cationic dendrimers based nanogels feature great potential in targeted DXM delivery and neutralizing cfDNA in the inflamed kidney, thereby alleviating the progression of LN.

In this study, we utilized a third-generation poly-lysine dendrimer (G3K) nanogel as the preferred nanocarrier for delivering DXM and as a cationic scavenger of cfDNA for the treatment of LN. The nanogel carriers, renowned for their outstanding biocompatibility attributed to their peptide-based natural composition, were synthesized by employing dithio-bis-(succinimidyl propionate) (DSP) to crosslink generation 3 polylysine (G3K) precursors. The resultant cationic nanogels (G3DSP) were demonstrated to be readily endocytosed by macrophages and disrupt the interaction between cfDNA and TLR9, showing competitive DNA binding affinity and stronger blockade of inflammation *in vitro*. In addition, the high levels of reactive oxygen species (ROS) in inflamed cells can accelerate the degradation of nanogels, contributing to the responsive drug release capacity of G3DSP. Moreover, after intravenous injecting G3DSP nanogels into MLR/lpr mice, these cationic nanogels displayed preferential accumulation and longer retention in the inflamed kidney. Especially, by loading DXM into the G3DSP nanogels (DXM@G3DSP), they exhibited significant cfDNA scavenging ability and targeted drug delivery property in vivo, thereby effectively preventing LN and alleviating disease symptoms. These findings underscore the promising role of cationic nanogels in treating LN and suggest a refined approach for the application of DNA scavengers.

2. Results and discussion

2.1. Fabrication of DXM-loaded cfDNA scavenger nanogel with renal homing ability

The preparation of cationic nanogel cfDNA scavengers was carried out using poly (L-lysine, K) dendrimers (G3K) (Fig. 1). A previously described procedure was used to successfully manufacture G3K with a precise molecular structure [30,31,45]. The synthesis of G3K was verified using the ^{1}H NMR spectrum (Fig. S1) and Matrix-assisted laser desorption/ionization time-of-flight mass spectrum (MALDI-TOF-MS, Fig. S2).

^{1}H NMR spectra showed that G3DSP nanogels were successfully fabricated by crosslinking G3K with a disulfide-containing linker (DSP) (Figs. S3 and S4). Since the gel composition and charge density drive the nucleic binding performance, cationic dendritic generation 4 poly K (G4K), cationic linear chitosan (CS), and anionic alginate (ALG) were used to prepare G4DSP, CSDSP, and G3ALG nanogels respectively as controls. Transmission Electron Microscope (TEM) scanning revealed the well-defined spherical dendritic morphologies of G4DSP, G3DSP, and G3ALG nanogels (Fig. 2a–d). The hydrodynamic sizes of nanogels evaluated by dynamic light scattering (DLS) were about 100–250 nm with narrow distribution. Notably, G4DSP, G3DSP, and CSDSP showed a positive zeta potential (+10 to +70 mV), while G3ALG demonstrate a negative surface charge of −20mV (Fig. 2e).

The G3DSP nanogels could hold their shape after 7 days of PBS incubation (Fig. S5). Once the DSP-linked nanogels have been endocytosed, intracellular ROS can destroy the disulfide and hasten the dissolution of nanogels. Following a 12-h incubation with 1 mM H_2O_2, the cross-linked architecture was destabilized, leading to the dispersion of G3K dendrimer units within the aqueous solution and an expansion of G3DSP's hydrodynamic diameter to approximately 800 nm (Fig. 2f and g). This ROS–responsive degradation capability motivated us to select this biomaterial as multifunctional drug carriers for the combined therapy of LN.

Before proceeding with the biological assessment, the nanogels underwent co-cultivation with mouse macrophages (RAW 264.7 cells) to determine their cytocompatibility using the CCK-8 assay. The results indicated that G3DSP nanogel exhibited minimal cytotoxicity across all concentrations tested, up to a maximum of 500 μg/mL, whereas G4DSP nanogel may exhibit cytotoxic effects in the specific conditions and

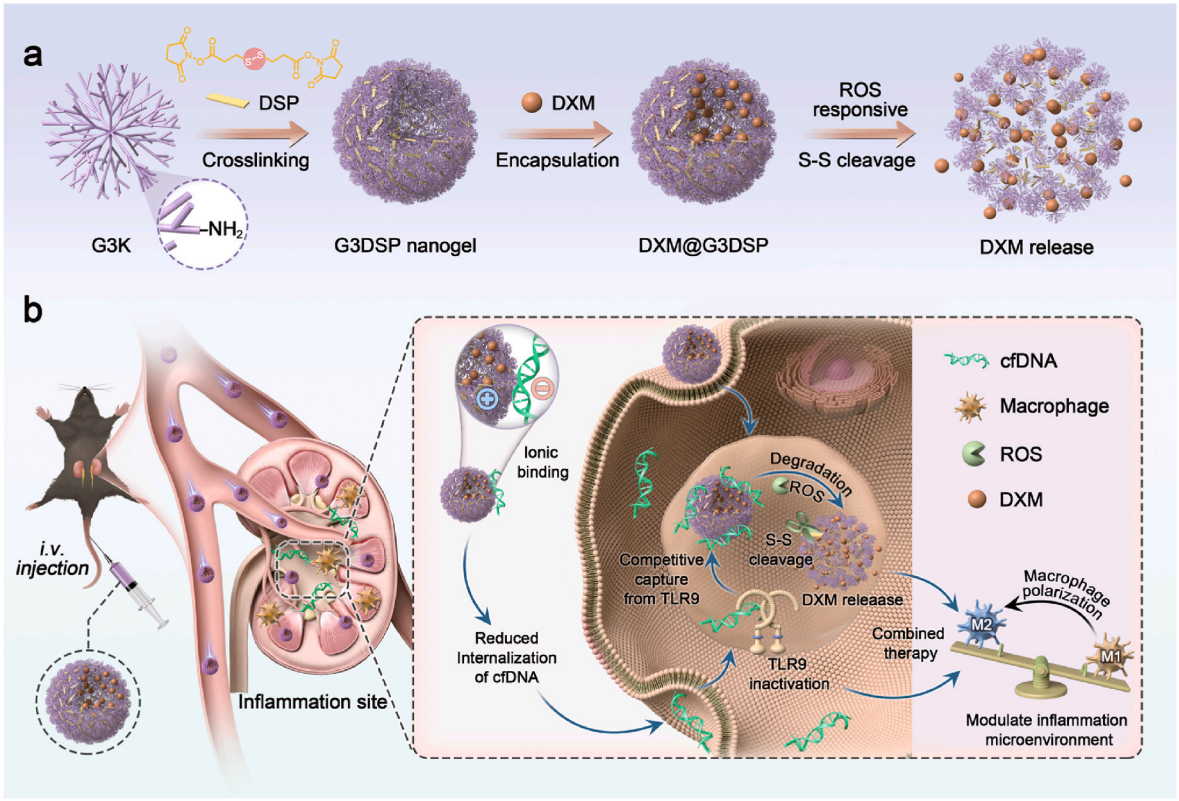

Fig. 1. Schematic illustration of DXM-loaded cfDNA scavenger nanogel with renal homing ability for LN treatment.

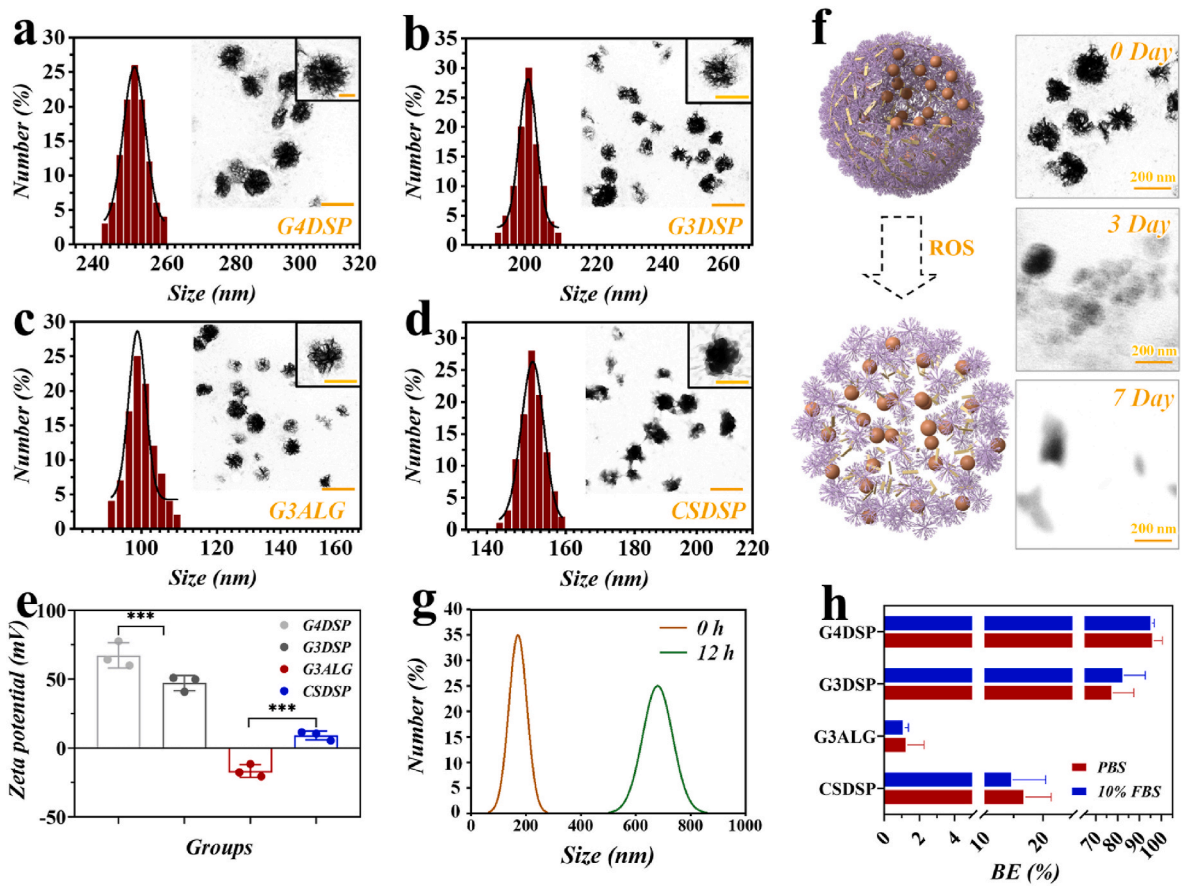

Fig. 2. The characterization of nanogels. a–d) Particle size distribution and TEM visuals for G4DSP, G3DSP, CSDSP, and G3ALG nanogels. e) Zeta potential of nanogels. f) TEM images of G3DSP nanogels after incubation in buffer containing 1 mM H_2O_2 for 0 days, 3 day, and 7 days. g) Changes in G3DSP nanogels' size distribution after a 12-h exposure to 1 mM H_2O_2 at 37 °C. h) Evaluation of nanogels' DNA trapping ability in PBS and 10 % FBS at a 1:1 nanogel-to-DNA mass ratio. Data are expressed as mean ± standard deviation (SD). Statistical significance was assessed using one-way ANOVA with Tukey post hoc tests, where *** signifies $P < 0.001$.

concentrations (Figs. S6 and S7). This favorable biocompatibility is likely due to the nanogels' composition of naturally sourced peptides and their protein-mimicking spherical architecture.

2.2. G3DSP demonstrates strong DNA scavenging ability

Having successfully confirmed their exceptional *in vitro* biocompatibility, we proceeded to investigate the DNA binding efficiency (BE) of nanogels using an ethidium bromide (EtBr) competitive binding assay. G4DSP and G3DSP nanogels demonstrated a higher DNA trapping affinity in both phosphate-buffered saline (PBS) at pH 7.4 and serum environments containing 10 % w/v fetal bovine serum (FBS), compared to CSDSP nanogels which exhibited a reduced surface charge density (Fig. 2h and Fig. S8). Notably, the anionic G3ALG nanogels lacked the capacity to bind negatively charged nucleic acids (NAs). This outcome suggests that upon intravenous injection and subsequent circulation in the bloodstream, the DNA scavenging ability of cationic nanogels remains unaffected by potential protein corona formation around the nanogels.

Subsequent investigations were focused on determining whether the cationic nanogels could impede TLR activation through competitive cfDNA neutralization. The positively charged G4DSP and G3DSP nanogels both demonstrated significant inhibitory effects on TLR9 activation, which was induced by the NA-based TLR agonist CpG-ODN2006 (Fig. 3a). In contrast, the anionic G3ALG nanogels exhibited minimal interference with TLR activation. Additionally, it was observed that none of the nanogels responded to TLR stimulation that was mediated by a non-NA activator, specifically the tri-acylated lipopeptide Pam3CSK4.

Following this, we delved into the potential mechanism of inflammation suppression via cellular uptake. We co-incubated Quasar 670-labeled CpG-ODN2006 (simulation of cfDNA) with FITC-labeled nanogels and RAW264.7 cells for a duration of 12 h (Fig. S9). The intracellular and extracellular movements of these compounds were meticulously monitored using Confocal Laser Scanning Microscopy (CLSM) at intervals of 4, 8, and 12 h. The introduction of G3DSP nanogels resulted in a marked decrease in the uptake of cfDNAs within the cells (Fig. S10), indicating that the cationic nanogels possess the ability to identify and sequester extracellular inflammatory cfDNAs, thereby reducing their internalization.

2.3. Competitive binding ability of G3DSP toward internalized cfDNA

In the experiments described, cells were exposed to nanogels and CpG simultaneously. However, under practical conditions, pathogenic cfDNAs might be absorbed by immune cells before therapeutic agents can act. To simulate this, CpG was first incubated with Ramos Blue™ reporter cells for 4 h, then any unbound CpG was thoroughly removed before introducing G3DSP nanogels. At 250 μg/mL, G3DSP nearly completely inhibited TLR9 activation. Remarkably, even at a reduced concentration of 25 μg/mL, TLR9 activation was suppressed by 60 %, showcasing G3DSP's dose-responsive antagonistic properties against TLR9 (Fig. S11).

Further studies to verify the competitive binding of nanogels to cfDNAs already inside cells involved tracking Quasar 670-labeled CpG

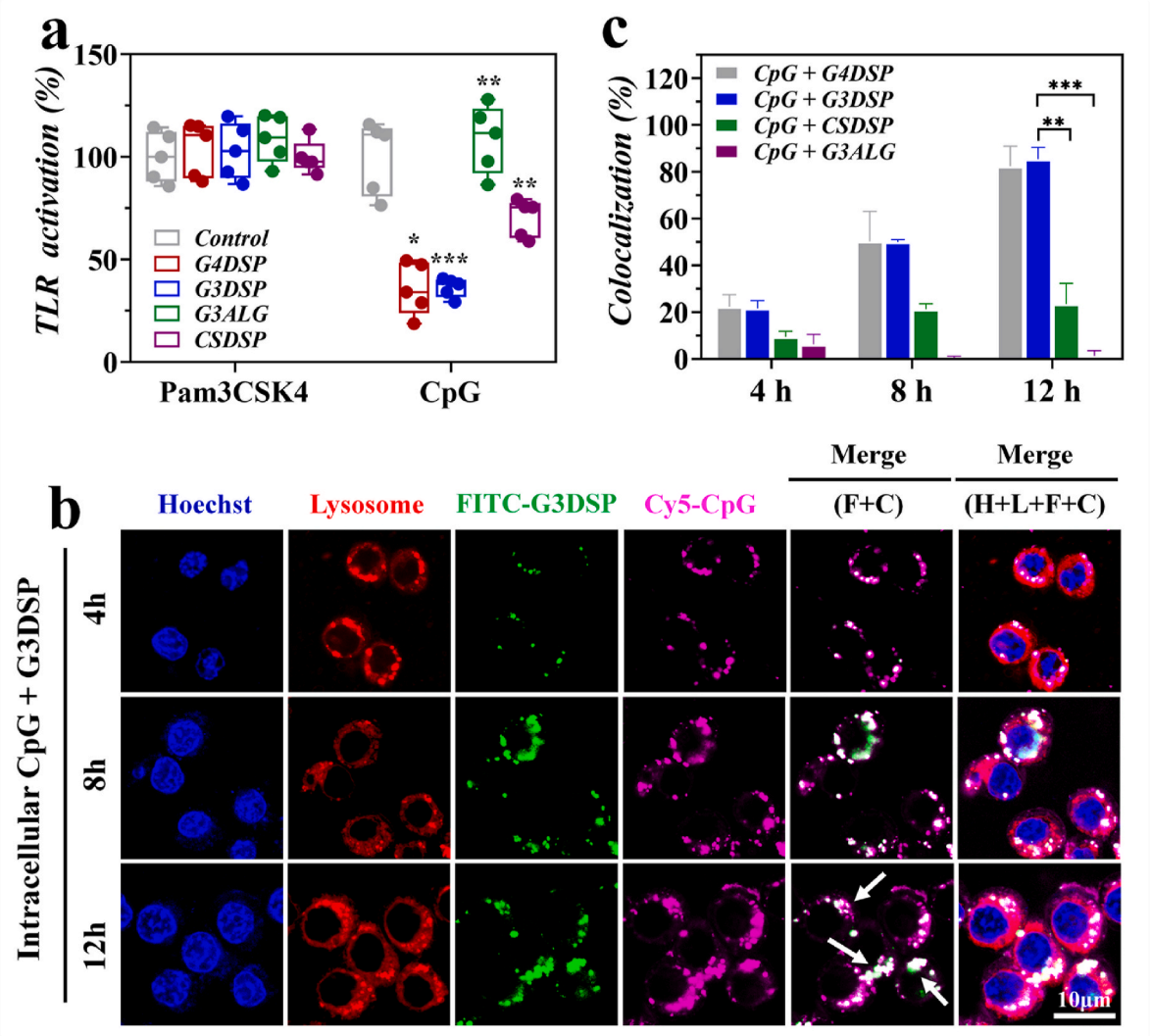

Fig. 3. Modulation of cellular inflammatory response by nanogels through cfDNA binding. a) The nanogels effectively downregulate NA-driven TLR9 activation in Ramos Blue™ cells, showcasing their potential in inflammatory response control. b) Time-lapse analysis of intracellular transport reveals the colocalization of Quasar 670-labeled CpG and FITC-labeled cationic G3DSP nanogels within RAW264.7 cells. The white arrows pinpoint the colocalization sites. Key: DAPI (D), Lysosome Tracker (L), FITC-labeled G3DSP (F), and Quasar 670-labeled CpG. c) The colocalization ratio, representing the interaction between Quasar 670-CpG and various FITC-cationic nanogels over time, was quantified using Image J. This ratio compares the colocalization area (white spots) to the total relevant area (green and purple spots). The data are presented as mean ± SD, with statistical significance determined by one-way ANOVA and subsequent Tukey post hoc tests, where * indicates $0.01 < P < 0.05$, ** signifies $0.001 < P < 0.01$, and *** denotes $P < 0.001$.

2006 and FITC-labeled G3DSP nanogels. Initial absorption of CpG by endolysosomes within 4 h suggested TLR9 engagement (Fig. 3b and Fig. S12). After the removal of CpG, G3DSP cationic nanogels were added, and their colocalization within cells was observed for 12 h. A pronounced accumulation of nanogels within the endolysosomal compartments was noted, forming a distinctive white punctate pattern. In contrast, G3ALG and CSDSP nanogels showed minimal interaction with CpG, even after 12 h (Fig. 3c and Fig. S13).

2.4. G3DSP promotes macrophage differentiation to anti-inflammatory M2 subtype

As the overproduction of ROS is the main cause of activation of macrophages, we investigated the *in vitro* ROS-scavenging ability of nanogels. Confocal microscopy results revealed that G3DSP nanogels can efficiently eliminate the overproduced ROS in activated macrophages (Fig. 4a). Based on this, we assessed the M1-to-M2 macrophage phenotypic shift under an inflammatory condition. Macrophages exhibiting the M1 phenotype are known to secrete various inflammatory cytokines in LN, potentially accelerating the progression of SLE. A promising therapeutic strategy for LN involves shifting macrophages from the M1 phenotype to the M2 phenotype, characterized by the markers iNOS (M1) and CD206 (M2). The efficacy of cationic nanogels in promoting M2 polarization was evaluated using mouse bone marrow-derived macrophages (BMDMs). BMDMs treated with G3DSP displayed an increased presence of CD206 and a significant reduction in iNOS levels, as determined by immunofluorescent staining of these specific cell surface markers, signifying a successful shift from M1 to M2 phenotype (Fig. 4b and c). In contrast, G3ALG and CSDSP demonstrated a limited capacity to reprogram macrophages.

Additionally, a panel of genes linked to pro-inflammatory and anti-inflammatory mechanisms, such as TNF-α, IL-6, Arg-1, and IL-10, were quantified using qRT-PCR. Relative to the control, macrophages cultured with G3DSP nanogels exhibited a pronounced reduction in the mRNA expression of TNF-α and IL-6, alongside an increase in Arg-1 and IL-10 levels (Fig. 4d). This pattern was echoed in the supernatant, where enzyme-linked immunosorbent assay (ELISA) confirmed the diminished release of pro-inflammatory cytokines and an elevated presence of the

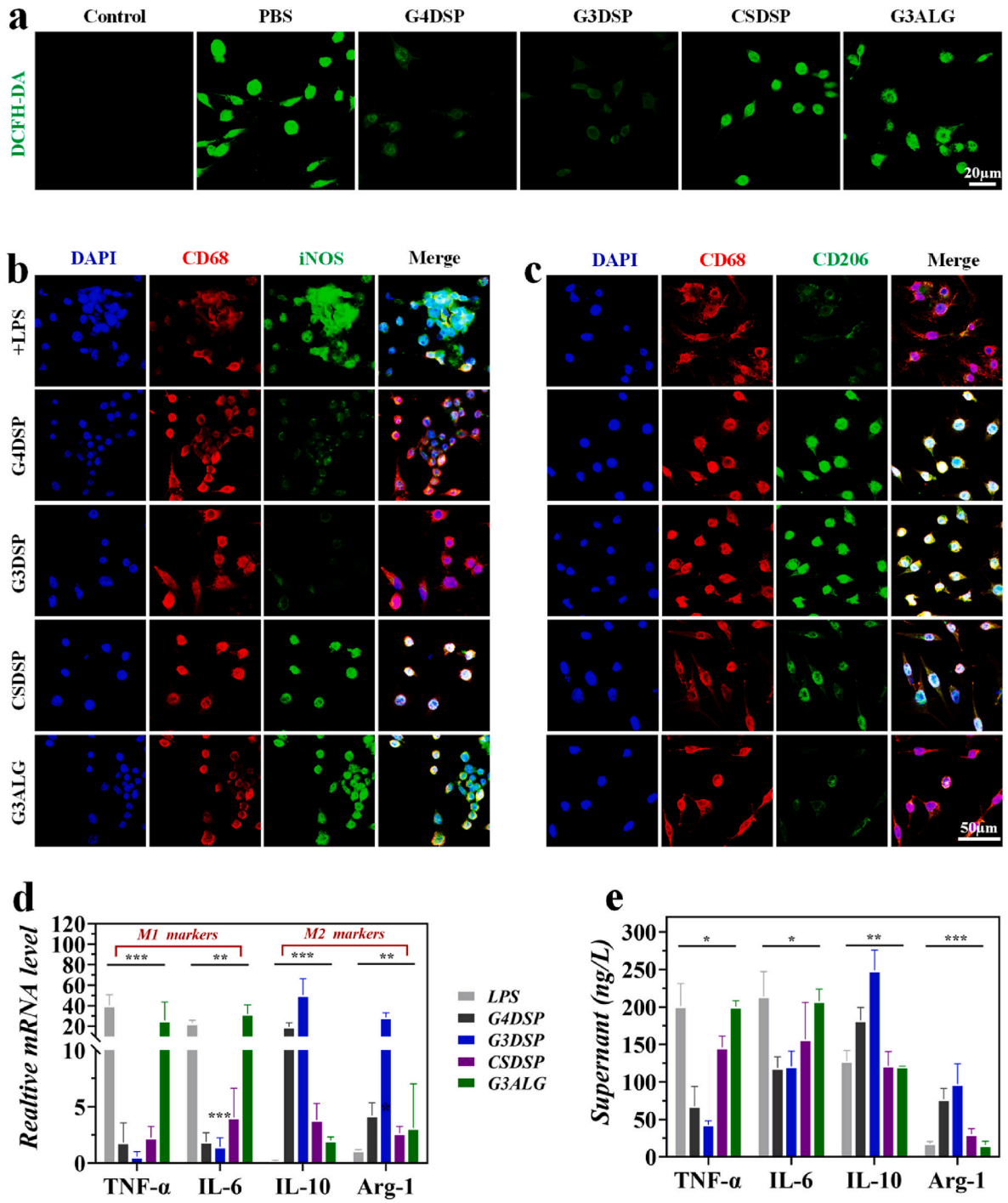

Fig. 4. Induction of M1 to M2 macrophage polarization *in vitro* by nanogels. a) In vitro ROS-scavenging of nanogels confirmed by confocal microscopy. b) and c) Immunofluorescence staining showcases the macrophage landscape: CD68 (universal macrophage marker in red), iNOS (M1 marker in green), CD206 (M2 marker in green), and cell nuclei (in blue). d) Quantitative real-time PCR (qRT-PCR) analysis reveals the mRNA expression levels of M1 markers (IL-6 and TNF-α) and M2 markers (Arg-1 and IL-10) in activated macrophages. e) Evaluation of pro-inflammatory and anti-inflammatory cytokines in the supernatant of BMDMs treated with nanogels. The data are presented as mean ± standard deviation (SD). Statistical significance was determined in comparison to the control group, using one-way ANOVA with subsequent Tukey post hoc tests, where * indicates $0.01 < P < 0.05$, ** signifies $0.001 < P < 0.01$, and *** denotes $P < 0.001$.

anti-inflammatory cytokine IL-10 in BMDMs treated with G3DSP (Fig. 4e). These findings collectively affirm the anti-inflammatory properties of G3DSP, which appears to facilitate the transition of macrophages to the anti-inflammatory M2 phenotype.

2.5. G3DSP achieves an extremely fast targeting accumulation in kidney of MRL/lpr mice

While the ability of cationic nanogels to identify and neutralize pathogenic cfDNAs has been established *in vitro*, their efficacy in targeting within a living organism was yet to be determined. To investigate this, we employed near-infrared fluorescence (NIRF) imaging to track the distribution of Alexa Flour 750-labeled nanogels (Fig. S14) in MRL/

lpr mice following intravenous (i.v.) injection. Upon organ analysis at 2- and 24-h post-treatment, we observed a pronounced accumulation of G4DSP and G3DSP nanogels in the kidneys (Fig. 5a, b, and c), suggesting a preferential accumulation of nanogels with a higher positive charge density in inflamed renal tissue. Remarkably, the G3DSP nanogels exhibited a unique ability to localize selectively to the kidneys without dispersing to other organs.

Furthermore, the signal intensity of G4DSP and G3DSP nanogels persisted robustly even 24 h after administration. In contrast, mice treated with G3ALG and CSDSP nanogels displayed a significant decrease in NIR signal, becoming nearly undetectable after 24 h, indicating that targeting precision and retention correlate with charge density (Fig. S15a). The mass of G3DSP nanogel per mass of kidney tissue after 24 h of each injection achieved 0.84 mg/g based on the standard curve that correlates nanogel fluorescence intensity to concentration (Fig. S15b). Immunofluorescence analysis of tissue sections further confirmed the renal homing ability of cationic dendrimer nanogels (Fig. 5d and Fig. S15c). The observed targeting phenomenon of the cationic nanogels is likely due to the minor vascular leakage in the renal system and the accumulation of negatively charged cfDNA in the inflamed kidneys of MRL/lpr mice.

2.6. G3DSP relieves SLE progression of MRL/lpr mice

Combinational SLE treatment is thought to be a potential method for achieving synergistic therapeutic benefits while minimizing medication dosage and adverse effects. In this study, we used a synergistic combination of DXM, a traditional corticosteroid widely used in clinical autoimmune disorders, and G3DSP, an cfDNA scavenger. The DXM was loaded into the network of G3DSP nanogel during crosslinking process, termed as DXM@G3DSP, to improve the poor water solubility of DXM. The drug loading content (DLC) and drug loading efficiency (DLE) of

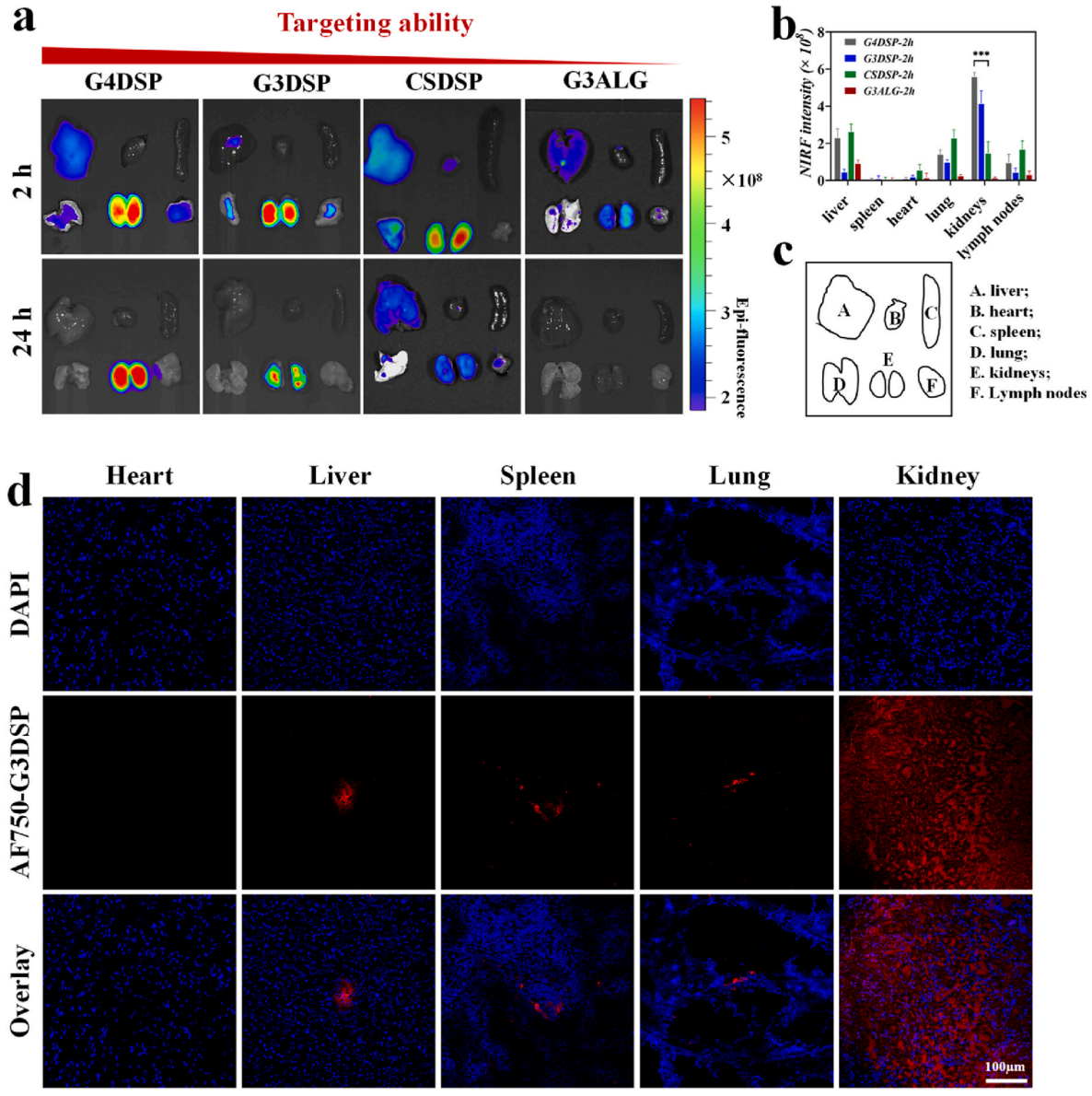

Fig. 5. Mechanistic insights into GSDSP's therapeutic efficacy in LN Treatment. a) Distribution mapping of nanogels within extra-articular tissues and joints, captured at 2- and 24-h post-injection using ex vivo NIRF imaging. b) Analysis of the average NIRF intensity from the cationic nanogels in an ex vivo distribution study conducted on MRL/lpr mice, measured 2 h following intravenous injection. c) A). liver; B). heart; C). spleen; D). lung; E). kidneys; F). lymph nodes. d) Various organs (heart, liver, spleen, lung, and kidney) in the G3DSP group were preserved, sectioned, and DAPI-stained 24 h after nanogel administration. Immunofluorescence images illustrate nanogel localization. DAPI staining is shown in blue, and nanogels are depicted in red. Data were presented as mean ± SD. Statistical significance was determined in comparison to the G3ALG group, using one-way ANOVA with subsequent Tukey post hoc tests, where *** denotes $P < 0.001$.

DXM were determined as 19.5 % and 91.7 %. The drug release patterns of DXM from DXM@G3DSP were then assessed in the absence and presence of ROS. The release curve demonstrated that the DXM was slowly and constantly released from nanogels at both pH values (Fig. S16). However, nearly 90 % of the DXM was released within 7 days at in the present of ROS and only 65 % at physiological environment, indicating the desired endo-lysosomal degradation of DXM@G3DSP.

Following the onset of lupus when the mice were 10 weeks old, a dose of 25 mg/kg of body weight of cationic nanogels was injected intravenously once a week to treat LN for 4 weeks (Fig. 6a). The specific skin lesions in the facial region exhibited a significant reduction in mice from the DXM@G3DSP group, resulting in a final nanogel mass ratio to kidney of 0.28 mg/g after treatment (Fig. 6b and Fig. S17). In accordance with the weight statistics, the DXM@G3DSP group had significantly smaller spleens and lymph nodes than the other groups (Fig. 6c–f). Both DXM@G3DSP and G3DSP nanogels were more effective in capturing and neutralizing cfDNAs in the bloodstream (Fig. 6g), likely due to their enhanced nucleic acid binding affinity and prolonged in vivo retention. Conversely, treatments with G3ALG and CSDSP, which lacked positive charges, showed only a slight decrease in systemic cfDNA levels. This underscores a direct link between cfDNA reduction and the alleviation of LN disease activity. While cfDNA is adsorbed by nanogels, it can still be partially internalized by renal cells alongside the nanogels. To attenuate the effects of cfDNA, future studies may explore loading protein gene silencing agents like siRNA or DNAzyme into the nanogels [46,47].

In SLE, multi-organ dysfunction is often accompanied by elevated levels of autoantibodies, including blood urea nitrogen (BUN), anti-dsDNA antibodies, and serum creatinine. The BUN levels were significantly higher in the serum of mice treated with PBS, G3ALG, and CSDSP, as depicted in Fig. 6h. In stark contrast, the DXM@G3DSP-treated mice displayed markedly lower levels of BUN. Further analysis of the DXM@G3DSP group revealed a substantial improvement in anti-dsDNA Abs and creatinine levels, which are critical indicators of renal function (Fig. 6i and j). Additionally, ELISA results indicated that post-treatment levels of inflammatory cytokines such as TNF-α, IL-6, and TGF-β were significantly reduced (Fig. S18). These outcomes collectively affirm the efficacy of DXM@G3DSP nanogels in treating LN and potentially other related clinical conditions.

LN stands as a critical marker for adverse outcomes in SLE, often leading to renal failure, the primary cause of mortality among SLE patients. Characterized by the accumulation of immune complexes and inflammation within the kidney's glomeruli and tubulointerstitial areas, LN presents a formidable challenge. To evaluate its therapeutic potential, DXM@G3DSP was subjected to further scrutiny in LN treatment. Compared to the control and other nanogel groups (PBS, G3ALG, CSDSP,

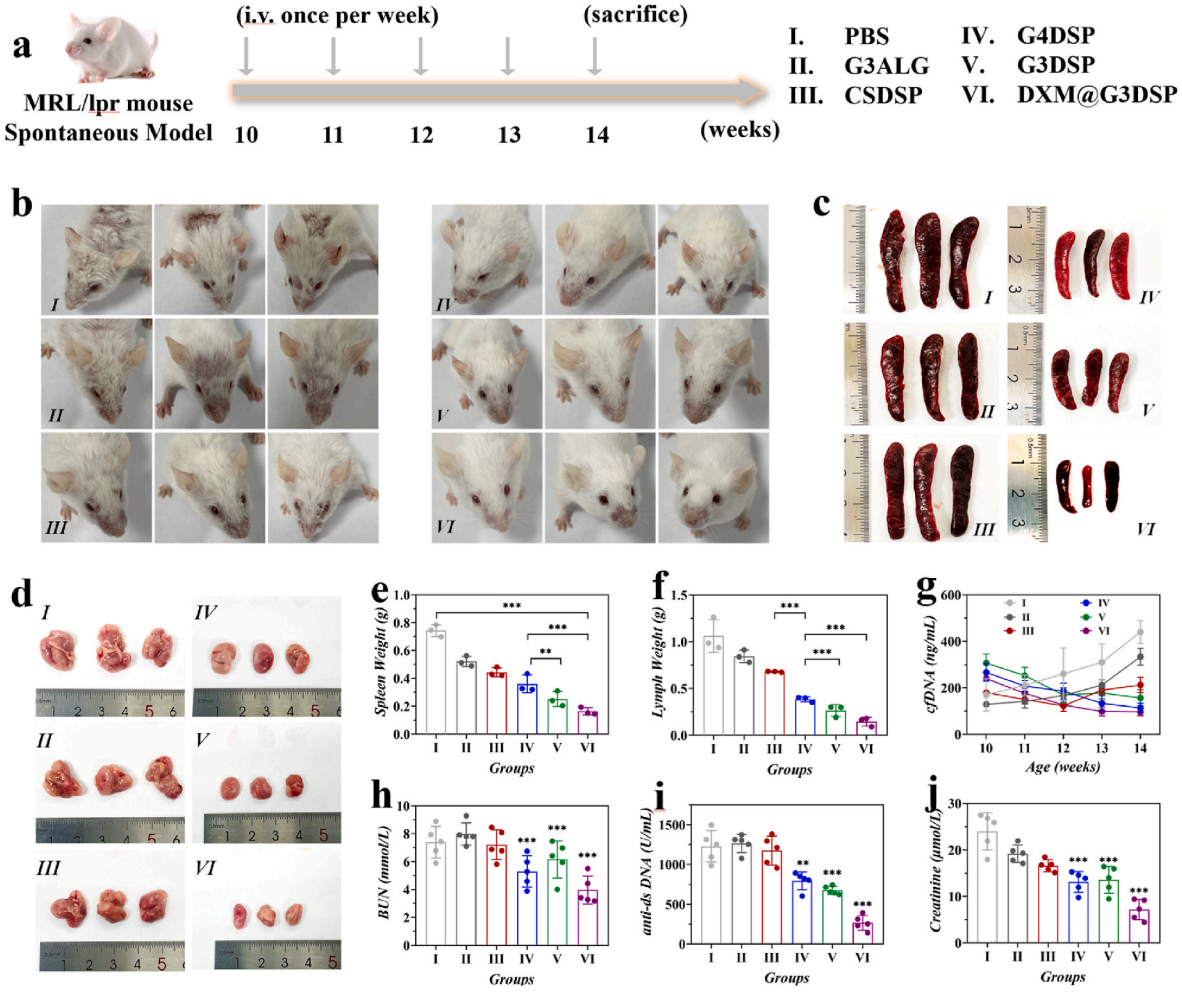

Fig. 6. Therapeutic impact of DXM@G3DSP on LN progression. a) Timeline showcasing the treatment schedule for MRL/lpr mice. b) Visual analysis of facial skin lesions at the 14-week mark. c) and e) Comparative images and data for spleen size across different treatment groups: PBS (I), G3ALG (II), CSDSP (III), G4DSP (IV), G3DSP (V), and DXM@G3DSP (VI). d) and f) Lymph node assessments, presented visually and quantitatively, for the same groups. g) Tracking serum cfDNA levels post-nanogel treatment at designated intervals. h) BUN, i) anti-dsDNA antibodies, and j) serum creatinine measurements, indicating renal function in treated mice. Data are expressed as mean ± standard error of the mean (s.e.m.). Statistical significance was determined using one-way ANOVA with subsequent Tukey post hoc tests, where * denotes $0.01 < P < 0.05$, ** indicates $0.001 < P < 0.01$, and *** signifies $P < 0.001$.

and G4DSP), histological analysis via H&E staining of the G3DSP group showed reduced glomerular enlargement, cellular infiltration, and glomerulonephritis (Fig. 7a). Notably, DXM@G3DSP treatment led to a stark inhibition of mesangial cell proliferation within the glomerulus (Fig. 7b), indicating a substantial mitigation of glomerular inflammation. The DXM@G3DSP group also exhibited the lowest levels of IgG and C3 deposits, suggesting that the dual-action therapy effectively curtailed the accumulation of glomerular immune complexes and ameliorated renal pathology in MRL/lpr mice (Fig. 7c and d). Pathological kidney scores further corroborated these findings, with the highest scores observed in the PBS group, followed by G3ALG, CSDSP, G3DSP, G4DSP, and the lowest in the DXM@G3DSP group (Fig. S19). Collectively, these results underscore the enhanced efficacy of DXM@G3DSP treatment over the use of nanogels alone.

The clinical application of cationic biomaterials is often hindered by their intrinsic toxicity. Mitigating these adverse effects while preserving their function as cfDNA scavengers presents a significant challenge. The DXM@G3DSP formulation, however, has shown promising therapeutic effects in mitigating the progression of LN, coupled with minimal organ toxicity (as evidenced in Fig. S20), aligning with previous *in vitro* findings. Moreover, the hepatotoxicity and nephrotoxicity markers—alanine aminotransferase (ALT), alkaline phosphatase (ALP), aspartate aminotransferase (AST), creatinine, uric acid, and urea—remained within normal ranges in MRL/lpr mice treated with nanogels (Fig. S21), indicating exceptional long-term biocompatibility. This favorable profile may be attributed to the nanogels' composition of natural peptides and their targeted distribution to inflamed kidneys, which enables localized cfDNA scavenging and alleviates LN symptoms without widespread side effects.

Synthesizing data from both *in vitro* and in vivo studies, we propose a mechanism for the DXM@G3DSP nanodrug system (Fig. 8). The nanogels' positive surface charge facilitates the binding and neutralization of anionic cfDNA via electrostatic interactions. This binding impedes the intracellular movement of cfDNA, preventing it from activating DNA sensors like TLR9 within the endolysosomes [48]. By clearing cfDNA, TLR9 activation and subsequent signaling through MyD88 and TRAF6 are reduced, leading to decreased phosphorylation and degradation of IκBα, an NFκB inhibitor. Consequently, NFκB's nuclear translocation and the expression of pro-inflammatory genes are inhibited, diminishing inflammation. Additionally, the DXM released from the nanogels serves as immunomodulatory ligands, competitively binding to receptors and curtailing the release of pro-inflammatory cytokines in LN. This dual anti-inflammatory action disrupts critical pathways in LN pathogenesis. In essence, DXM@G3DSP nanogels offer a comprehensive approach to modulating inflammatory responses in LN, underscoring their potential as a therapeutic option and providing valuable insights into their mode of action.

3. Conclusion

In this paper, we proposed a desired nanogel to serve as cfDNA scavenger and targeted DXM carrier for LN treatment. By using G3K, G4K, CS, and ALG to prepare G3DSP, G4DSP, CSDSP, and G3ALG, respectively, we confirmed their biocompatibility and compared their DNA scavenging ability and TLR inhibitory capacity. Among them, G3DSP showed superior DNA binding capacity, realized competitive colocalization with cfDNA in lysosomes, and inhibited TLR9 activation *in vitro*. After systemic administrating G3DSP to MRL/lpr mice, these nanogels displayed preferential biodistribution and longer retention in inflamed kidney. Furthermore, by loading DXM into the cavities of G3DSP nanogels, the DXM@G3DSP could effectively prevent LN engendered by proinflammatory nucleic acids and alleviate SLE symptoms through synergistic treatments. Therefore, our study shed new light on the promising prospect of cationic peptide dendrimer nanogels for cfDNA clearance and targeted corticosteroids delivery in SLE treatment.

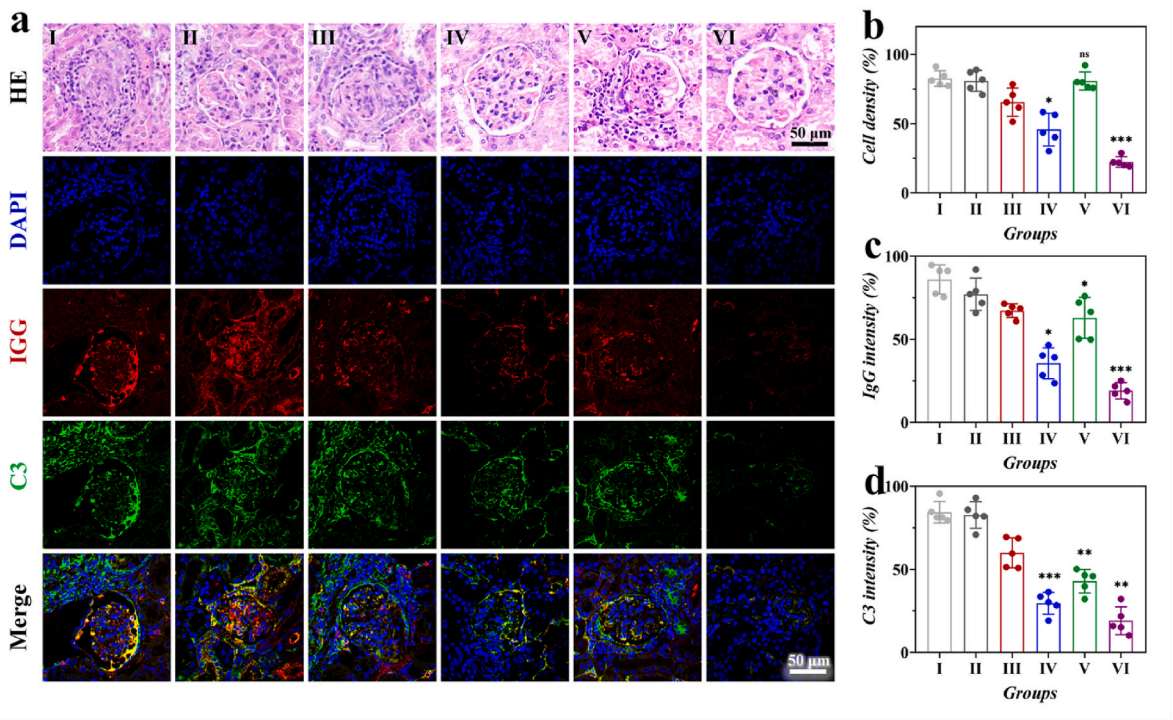

Fig. 7. Histological analysis of LN treatment via various nanogels. a) Histological examination of renal sections using H&E staining, along with IgG and C3 immunofluorescence, across various treatment groups: PBS (I), G3ALG (II), CSDSP (III), G4DSP (IV), G3DSP (V), and DXM@G3DSP (VI). b) Assessment of mesangial cell density within the glomerulus. c) and d) Quantification of IgG and C3 fluorescence intensity in the glomerulus, performed with Image J software. Data are represented as mean ± s.e.m. Statistical significance was determined through one-way ANOVA and subsequent Tukey post hoc tests, where * indicates $0.01 < P < 0.05$, ** denotes $0.001 < P < 0.01$, and *** signifies $P < 0.001$.

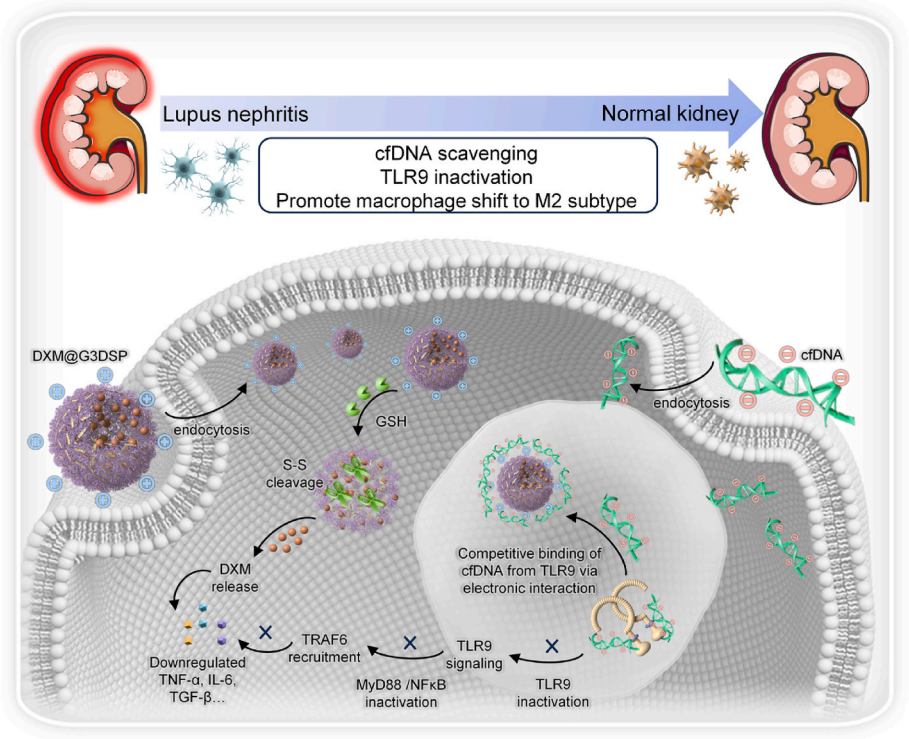

Fig. 8. Proposed mechanism of DXM@G3DSP for anti-inflammatory activity in LN.

Ethics approval and consent to participate

All animal experiments were performed according to the Ethics Committee of Drum Tower Hospital and the approval number issued by the Laboratory Animal Welfare Ethics Committee of Drum Tower Hospital was 2021AE01008.

CRediT authorship contribution statement

Haofang Zhu: Writing – original draft, Investigation, Formal analysis, Data curation. **Danqing Huang:** Investigation. **Min Nie:** Methodology. **Yuanjin Zhao:** Writing – review & editing, Supervision. **Lingyun Sun:** Writing – review & editing, Supervision, Project administration, Funding acquisition.

Declaration of competing interest

Yuanjin Zhao is an editorial board member for Bioactive Materials and was not involved in the editorial review or the decision to publish this article. All authors declare that there are no competing interests.

Acknowledgments

This work was supported by the National Key R&D Program of China (2020YFA0710800), the Key Program of National Natural Science Foundation of China (grant no. 81930043, 82330055 and 32401109), and the Research Fund of Anhui Institute of translational medicine (2023zhyx-C18).

Appendix A. Supplementary data

Supplementary data to this article can be found online at https://doi.org/10.1016/j.bioactmat.2024.08.030.

References

[1] A. Jalal, T. Li, The evolving landscape of immune-mediated glomerular diseases, Nat. Rev. Nephrol. 19 (2) (2023) 81–82.
[2] S.J. Allison, Determining treatment response in lupus nephritis, Nat. Rev. Nephrol. 18 (9) (2022) 543, 543.
[3] M.T. Lotze, H.J. Zeh, A. Rubartelli, L.J. Sparvero, A.A. Amoscato, N.R. Washburn, M.E. DeVera, X. Liang, M. Tör, T. Billiar, The grateful dead: damage-associated molecular pattern molecules and reduction/oxidation regulate immunity, Immunol. Rev. 220 (1) (2007) 60–81.
[4] F.J. Barrat, T. Meeker, J. Gregorio, J.H. Chan, S. Uematsu, S. Akira, B. Chang, O. Duramad, R.L. Coffman, Nucleic acids of mammalian origin can act as endogenous ligands for Toll-like receptors and may promote systemic lupus erythematosus, J. Exp. Med. 202 (8) (2005) 1131–1139.
[5] E. Rykova, A. Sizikov, D. Roggenbuck, O. Antonenko, L. Bryzgalov, E. Morozkin, K. Skvortsova, V. Vlassov, P. Laktionov, V. Kozlov, Circulating DNA in rheumatoid arthritis: pathological changes and association with clinically used serological markers, Arthritis Res. Ther. 19 (1) (2017) 85.
[6] T. Hashimoto, K. Yoshida, N. Hashimoto, A. Nakai, K. Kaneshiro, K. Suzuki, Y. Kawasaki, N. Shibanuma, A. Hashiramoto, Circulating cell free DNA: a marker to predict the therapeutic response for biological DMARDs in rheumatoid arthritis, International Journal of Rheumatic Diseases 20 (6) (2017) 722–730.
[7] F.J. Barrat, T. Meeker, J.H. Chan, C. Guiducci, R.L. Coffman, Treatment of lupus-prone mice with a dual inhibitor of TLR7 and TLR9 leads to reduction of autoantibody production and amelioration of disease symptoms, Eur. J. Immunol. 37 (12) (2007) 3582–3586.
[8] Q. Guo, C. Chen, Z. Wu, W. Zhang, L. Wang, J. Yu, L. Li, J. Zhang, Y. Duan, Engineered PD-1/TIGIT dual-activating cell-membrane nanoparticles with dexamethasone act synergistically to shape the effector T cell/Treg balance and alleviate systemic lupus erythematosus, Biomaterials 285 (2022) 121517.
[9] Q. Xiao, X. Li, Y. Li, Z. Wu, C. Xu, Z. Chen, W. He, Biological drug and drug delivery-mediated immunotherapy, Acta Pharm. Sin. B 11 (4) (2021) 941–960.
[10] Z. Zhao, Z. Jia, K.W. Foster, X. Wei, F. Qiao, H. Jiang, Y. Jin, G. Li, N. Chen, G. Zhao, G.M. Thiele, J.L. Medlin, J.R. O'Dell, D. Wang, Dexamethasone prodrug nanomedicine (ZSJ-0228) treatment significantly reduces lupus nephritis in mice without measurable side effects - a 5-month study, Nanomedicine 31 (2021) 102302.
[11] L. Fan, X. Zhang, X. Liu, B. Sun, L. Li, Y. Zhao, Responsive hydrogel microcarrier-integrated microneedles for versatile and controllable drug delivery, Adv. Healthcare Mater. 10 (9) (2021) e2002249.
[12] T. Alexander, R. Sarfert, J. Klotsche, A.A. Kuehl, A. Rubbert-Roth, H.-M. Lorenz, J. Rech, B.F. Hoyer, Q. Cheng, A. Waka, A. Taddeo, M. Wiesener, G. Schett, G.-R. Burmester, A. Radbruch, F. Hiepe, R.E. Voll, The proteasome inhibitior bortezomib depletes plasma cells and ameliorates clinical manifestations of refractory systemic lupus erythematosus, Ann. Rheum. Dis. 74 (7) (2015) 1474–1478.

[13] Z. Jia, X. Wang, X. Wei, G. Zhao, K.W. Foster, F. Qiu, Y. Gao, F. Yuan, F. Yu, G. M. Thiele, T.K. Bronich, J.R. O'Dell, D. Wang, Micelle-forming dexamethasone prodrug attenuates nephritis in lupus-prone mice without apparent glucocorticoid side effects, ACS Nano 12 (8) (2018) 7663–7681.
[14] C. Zhao, L. Cai, M. Nie, L. Shang, Y. Wang, Y. Zhao, Cheerios effect inspired microbubbles as suspended and adhered oral delivery systems, Adv. Sci. 8 (7) (2021) 2004184.
[15] S.C. Funes, M. Rios, F. Gomez-Santander, A. Fernandez-Fierro, M.J. Altamirano-Lagos, D. Rivera-Perez, R. Pulgar-Sepulveda, E.L. Jara, D. Rebolledo-Zelada, A. Villarroel, J.C. Roa, J.P. Mackern-Oberti, A.M. Kalergis, Tolerogenic dendritic cell transfer ameliorates systemic lupus erythematosus in mice, Immunology 158 (4) (2019) 322–339.
[16] S. Edavalath, M.K. Rai, V. Gupta, R. Mishra, D.P. Misra, L. Gupta, V. Agarwal, Tacrolimus induces remission in refractory and relapsing lupus nephritis by decreasing P-glycoprotein expression and function on peripheral blood lymphocytes, Rheumatol. Int. 42 (8) (2022) 1347–1354.
[17] S. Cooray, H. Zhang, R. Breen, G. Carr-White, R. Howard, M. Cuadrado, D. D'Cruz, G. Sanna, Cerebral tuberculosis in a patient with systemic lupus erythematosus following cyclophosphamide treatment: a case report, Lupus 27 (4) (2018) 670–675.
[18] J.L. Kelliher, K.L. West, Q. Gong, J.W.C. Leung, Histone H2A variants alpha1-extension helix directs RNF168-mediated ubiquitination, Nat. Commun. 11 (1) (2020) 2462, 2462.
[19] J. Wu, F. Li, X. Hu, J. Lu, X. Sun, J. Gao, D. Ling, Responsive assembly of silver nanoclusters with a biofilm locally amplified bactericidal effect to enhance treatments against multi-drug-resistant bacterial infections, ACS Cent. Sci. 5 (8) (2019) 1366–1376.
[20] E.C. Wayne, C. Long, M.J. Haney, E.V. Batrakova, T.M. Leisner, L.V. Parise, A. V. Kabanov, Targeted delivery of siRNA lipoplexes to cancer cells using macrophage transient horizontal gene transfer, Adv. Sci. 6 (21) (2019) 1900582, 1900582.
[21] W. Chin, G. Zhong, Q. Pu, C. Yang, W. Lou, P.F. De Sessions, B. Periaswamy, A. Lee, Z.C. Liang, X. Ding, S. Gao, C.W. Chu, S. Bianco, C. Bao, Y.W. Tong, W. Fan, M. Wu, J.L. Hedrick, Y.Y. Yang, A macromolecular approach to eradicate multidrug resistant bacterial infections while mitigating drug resistance onset, Nat. Commun. 9 (1) (2018) 917, 917.
[22] T. Kawai, S. Akira, Toll-like receptors and their crosstalk with other innate receptors in infection and immunity, Immunity 34 (5) (2011) 637–650.
[23] T. Junt, W. Barchet, Translating nucleic acid-sensing pathways into therapies, Nat. Rev. Immunol. 15 (9) (2015) 529–544.
[24] F.J. Barrat, R.L. Coffman, Development of TLR inhibitors for the treatment of autoimmune diseases, Immunol. Rev. 223 (2008) 271–283.
[25] E.R. Kandimalla, L. Bhagat, D. Wang, D. Yu, T. Sullivan, N. La Monica, S. Agrawal, Design, synthesis and biological evaluation of novel antagonist compounds of Toll-like receptors 7, 8 and 9, Nucleic Acids Res. 41 (6) (2013) 3947–3961.
[26] J. Lee, J.W. Sohn, Y. Zhang, K.W. Leong, D. Pisetsky, B.A. Sullenger, Nucleic acid-binding polymers as anti-inflammatory agents, Proc. Natl. Acad. Sci. U. S. A. 108 (34) (2011) 14055–14060.
[27] E.K. Holl, K.L. Shumansky, G. Pitoc, E. Ramsburg, B.A. Sullenger, Nucleic acid scavenging polymers inhibit extracellular DNA-mediated innate immune activation without inhibiting anti-viral responses, PLoS One 8 (7) (2013).
[28] S. Jain, G.A. Pitoc, E.K. Holl, Y. Zhang, L. Borst, K.W. Leong, J. Lee, B.A. Sullenger, Nucleic acid scavengers inhibit thrombosis without increasing bleeding, Proc. Natl. Acad. Sci. U. S. A. 109 (32) (2012) 12938–12943.
[29] E.K. Holl, K.L. Shumansky, L.B. Borst, A.D. Burnette, C.J. Sample, E.A. Ramsburg, B.A. Sullenger, Scavenging nucleic acid debris to combat autoimmunity and infectious disease, Proc. Natl. Acad. Sci. U. S. A. 113 (35) (2016) 9728–9733.
[30] H. Zhu, X. Wu, R. Liu, Y. Zhao, L. Sun, ECM-inspired hydrogels with ADSCs encapsulation for rheumatoid arthritis treatment, Adv. Sci. (2023) e2206253.
[31] H. Zhu, B. Kong, M. Nie, C. Zhao, R. Liu, Y. Xie, Y. Zhao, L. Sun, ECM-inspired peptide dendrimer microgels with human MSCs encapsulation for systemic lupus erythematosus treatment, Nano Today 43 (2022) 101454.
[32] K. Luo, C. Li, G. Wang, Y. Nie, B. He, Y. Wu, Z. Gu, Peptide dendrimers as efficient and biocompatible gene delivery vectors: synthesis and in vitro characterization, J. Contr. Release 155 (1) (2011) 77–87.
[33] J. Wan, P.F. Alewood, Peptide-decorated dendrimers and their bioapplications, Angew Chem. Int. Ed. Engl. 55 (17) (2016) 5124–5134.
[34] R. Duncan, L. Izzo, Dendrimer biocompatibility and toxicity, Adv. Drug Deliv. Rev. 57 (15) (2005) 2215–2237.
[35] J. Zhou, Z. Zhang, J. Joseph, X. Zhang, B.E. Ferdows, D.N. Patel, W. Chen, G. Banfi, R. Molinaro, D. Cosco, N. Kong, N. Joshi, O.C. Farokhzad, C. Corbo, W. Tao, Biomaterials and nanomedicine for bone regeneration: progress and future prospects, Explorations 1 (2) (2021) 20210011.
[36] W. Chen, W. Tao, Precise control of the structure of synthetic hydrogel networks for precision medicine applications, MATTER 5 (1) (2022) 18–19.
[37] X. Xu, Y. Jian, Y. Li, X. Zhang, Z. Tu, Z. Gu, Bio-Inspired supramolecular hybrid dendrimers self-assembled from low-generation peptide dendrons for highly efficient gene delivery and biological tracking, ACS Nano 8 (9) (2014) 9255–9264.
[38] J. Chen, Z. Jiang, Y.S. Zhang, J. Ding, X. Chen, Smart transformable nanoparticles for enhanced tumor theranostics, Appl. Phys. Rev. 8 (4) (2021).
[39] T. Yong, X. Zhang, N. Bie, H. Zhang, X. Zhang, F. Li, A. Hakeem, J. Hu, L. Gan, H. A. Santos, X. Yang, Tumor exosome-based nanoparticles are efficient drug carriers for chemotherapy, Nat. Commun. 10 (2019).
[40] Y. Wang, J. Guo, X. Cao, Y. Zhao, Developing conductive hydrogels for biomedical applications, Smart Medicine 3 (1) (2024) e20230023.
[41] F. Lin, Y. Li, W. Cui, Injectable hydrogel microspheres in cartilage repair, Biomedical Technology 1 (2023) 18–29.
[42] S. Yang, F. Wang, H. Han, H.A. Santos, Y. Zhang, H. Zhang, J. Wei, Z. Cai, Fabricated technology of biomedical micro-nano hydrogel, Biomedical Technology 2 (2023) 31–48.
[43] M. Furtado, L. Chen, Z. Chen, A. Chen, W. Cui, Development of fish collagen in tissue regeneration and drug delivery, Engineered Regeneration 3 (3) (2022) 217–231.
[44] Z. Luo, J. Che, L. Sun, L. Yang, Y. Zu, H. Wang, Y. Zhao, Microfluidic electrospray photo-crosslinkable κ-Carrageenan microparticles for wound healing, Engineered Regeneration 2 (2021) 257–262.
[45] L. Wu, X. Cai, H. Zhu, J. Li, D. Shi, D. Su, D. Yue, Z. Gu, PDT-driven highly efficient intracellular delivery and controlled release of CO in combination with sufficient singlet oxygen production for synergistic anticancer therapy, Adv. Funct. Mater. 28 (41) (2018).
[46] J. Yan, X. Ma, D. Liang, M. Ran, D. Zheng, X. Chen, S. Zhou, W. Sun, X. Shen, H. Zhang, An autocatalytic multicomponent DNAzyme nanomachine for tumor-specific photothermal therapy sensitization in pancreatic cancer, Nat. Commun. 14 (1) (2023) 6905.
[47] J. Yan, R. Bhadane, M. Ran, X. Ma, Y. Li, D. Zheng, O.M.H. Salo-Ahen, H. Zhang, Development of Aptamer-DNAzyme based metal-nucleic acid frameworks for gastric cancer therapy, Nat. Commun. 15 (1) (2024) 3684.
[48] H. Zhu, B. Kong, J. Che, Y. Zhao, L. Sun, Bioinspired nanogels as cell-free DNA trapping and scavenging organelles for rheumatoid arthritis treatment, Proc. Natl. Acad. Sci. U. S. A. 120 (33) (2023) e2303385120.